Generation and tight focusing of hybridly polarized vector beams

Gilad M. Lerman,[1,*] Liron Stern,[1] and Uriel Levy[1,2]

[1]*Department of Applied Physics, The Benin School of Engineering and Computer Science, The Center for Nanoscience and Nanotechnology, The Hebrew University of Jerusalem, Jerusalem, 91904, Israel*
[2]*ulevy@cc.huji.ac.il*
**gilad.lerman@mail.huji.ac.il*

Abstract: We propose and experimentally demonstrate the generation of hybridly polarized beams by transmitting radially polarized light through a wave plate. We show that such beams span a closed circle on the surface of the Poincaré sphere whose center coincides with the center of the sphere. In addition we numerically investigate the field and energy density distribution across the focal plane of a high NA lens illuminated by such a hybrid beam. The results show an interesting polarization distribution with 3D orientation and space variant ellipticity. This kind of polarization distributions may be used for a variety of applications, e.g. particle orientation analysis, microscopy and in atomic systems.

OCIS codes: (260.5430) Polarization; (300.0300) Spectroscopy; (180.0180) Microscopy.

References and links

1. Q. Zhan, "Cylindrical vector beams: from mathematical concepts to applications," Adv. Opt. Photon. **1**(1), 1–57 (2009).
2. K. S. Youngworth, and T. G. Brown, "Focusing of high numerical aperture cylindrical-vector beams," Opt. Express **7**(2), 77–87 (2000).
3. Q. Zhan, and J. R. Leger, "Focus shaping using cylindrical vector beams," Opt. Express **10**(7), 324–331 (2002).
4. R. Dorn, S. Quabis, and G. Leuchs, "Sharper focus for a radially polarized light beam," Phys. Rev. Lett. **91**(23), 233901 (2003).
5. G. M. Lerman, and U. Levy, "Effect of radial polarization and apodization on spot size under tight focusing conditions," Opt. Express **16**(7), 4567–4581 (2008).
6. E. Descrovi, L. Vaccaro, L. Aeschimann, W. Nakagawa, U. Staufer, and H.-P. Herzig, "Optical properties of microfabricated fully-metal-coated near-field probes in collection mode," J. Opt. Soc. Am. A **22**(7), 1432–1441 (2005).
7. V. G. Niziev, and A. V. Nesterov, "Influence of beam polarization on laser cutting efficiency," J. Phys. D Appl. Phys. **32**(13), 1455–1461 (1999).
8. W. S. Mohammed, A. Mehta, M. Pitchumani, and E. G. Johnson, "Selective Excitation of the TE01 Mode in Hollow-Glass Waveguide Using a Subwavelength Grating," IEEE Photon. Technol. Lett. **17**(7), 1441–1443 (2005).
9. S. Quabis, R. Dorn, M. Eberler, O. Glöckl, and G. Leuchs, "Focusing light to a tighter spot," Opt. Commun. **179**(1-6), 1–7 (2000).
10. M. Born, and E. Wolf, *Principles of Optics: Electromagnetic theory of propagation, interference and diffraction*, 7th ed. (Cambridge University Press, 1999) pp. 24–38.
11. X. L. Wang, Y. Li, J. Chen, C. S. Guo, J. Ding, and H. T. Wang, "A new type of vector fields with hybrid states of polarization," Opt. Express **18**(10), 10786–10795 (2010).
12. G. Milione, and R. R. Alfano, Cylindrical vector beam transformations and hybrid vector beams" in Frontiers in Optics (FiO)/Laser Science (LS) (Optical Society of America, Washington, DC, 2010), paper FWC4.
13. G. Milione, H. I. Sztul, and R. R. Alfano, "Propagation of a hybrid vector polarization beam in a uniaxial crystal," Proc. SPIE **7613**, 76130I (2010).
14. Y. Tokizane, K. Oka, and R. Morita, "Supercontinuum optical vortex pulse generation without spatial or topological-charge dispersion," Opt. Express **17**(17), 14517–14525 (2009).
15. A. M. Beckley, T. G. Brown, and M. A. Alonso, "Full Poincaré beams," Opt. Express **18**(10), 10777–10785 (2010).
16. X. L. Wang, J. Ding, W. J. Ni, C. S. Guo, and H. T. Wang, "Generation of arbitrary vector beams with a spatial light modulator and a common path interferometric arrangement," Opt. Lett. **32**(24), 3549–3551 (2007).

#138361 - $15.00 USD Received 17 Nov 2010; revised 10 Dec 2010; accepted 10 Dec 2010; published 15 Dec 2010

17. G. Machavariani, Y. Lumer, I. Moshe, A. Meir, S. Jackel, and N. Davidson, "Birefringence-induced bifocusing for selection of radially or azimuthally polarized laser modes," Appl. Opt. **46**(16), 3304–3310 (2007).
18. M. A. Ahmed, A. Voss, M. M. Vogel, and T. Graf, "Multilayer polarizing grating mirror used for the generation of radial polarization in Yb:YAG thin-disk lasers," Opt. Lett. **32**(22), 3272–3274 (2007).
19. A. K. Spilman, and T. G. Brown, "Stress birefringent, space-variant wave plates for vortex illumination," Appl. Opt. **46**(1), 61–66 (2007).
20. Z. Bomzon, G. Biener, V. Kleiner, and E. Hasman, "Radially and azimuthally polarized beams generated by space-variant dielectric subwavelength gratings," Opt. Lett. **27**(5), 285–287 (2002).
21. T. Grosjean, D. Courjon, and M. Spajer, "An all-fiber device for generating radially and other polarized light beams," Opt. Commun. **203**(1-2), 1–5 (2002).
22. G. M. Lerman, and U. Levy, "Generation of a radially polarized light beam using space-variant subwavelength gratings at 1064 nm," Opt. Lett. **33**(23), 2782–2784 (2008).
23. M. Stalder, and M. Schadt, "Linearly polarized light with axial symmetry generated by liquid-crystal polarization converters," Opt. Lett. **21**(23), 1948–1950 (1996).
24. Y. Kozawa, and S. Sato, "Focusing property of a double-ring-shaped radially polarized beam," Opt. Lett. **31**(6), 820–822 (2006).
25. B. Hao, and J. Leger, "Experimental measurement of longitudinal component in the vicinity of focused radially polarized beam," Opt. Express **15**(6), 3550–3556 (2007).
26. N. Davidson, and N. Bokor, "High-numerical-aperture focusing of radially polarized doughnut beams with a parabolic mirror and a flat diffractive lens," Opt. Lett. **29**(12), 1318–1320 (2004).
27. E. Y. S. Yew, and C. J. R. Sheppard, "Tight focusing of radially polarized Gaussian and Bessel-Gauss beams," Opt. Lett. **32**(23), 3417–3419 (2007).
28. D. Biss, and T. Brown, "Cylindrical vector beam focusing through a dielectric interface," Opt. Express **9**(10), 490–497 (2001).
29. Y. Kozawa, and S. Sato, "Sharper focal spot formed by higher-order radially polarized laser beams," J. Opt. Soc. Am. A **24**(6), 1793–1798 (2007).
30. W. B. Chen, and Q. W. Zhan, "Three-dimensional focus shaping with cylindrical vector beams," Opt. Commun. **265**(2), 411–417 (2006).
31. X. L. Wang, J. Ding, J. Q. Qin, J. Chen, Y. X. Fan, and H. T. Wang, "Configurable three-dimensional optical cage generated from cylindrical vector beams," Opt. Commun. **282**(17), 3421–3425 (2009).
32. W. B. Chen, and Q. W. Zhan, "Diffraction limited focusing with controllable arbitrary three-dimensional polarization," J. Opt. **12**(4), 045707 (2010).
33. B. Richards, and E. Wolf, "Electromagnetic diffraction in optical systems II. Structure of the image field in an aplanatic system," Proc. R. Soc. Lond. A **253**(1274), 358–379 (1959).
34. G. M. Lerman, and U. Levy, "Tight focusing of space variant vector optical fields with no cylindrical symmetry of polarization," Opt. Lett. **32**, 2194–2196 (2007).
35. M. R. Beversluis, L. Novotny, and S. J. Stranick, "Programmable vector point-spread function engineering," Opt. Express **14**(7), 2650–2656 (2006).
36. F. K. Fatemi, and G. Beadie, "Imaging Atomic States Using Radially-Polarized Light," in Frontiers in Optics (FiO)/Laser Science (LS) (Optical Society of America, Washington, DC, 2010), paper FWP6.

1. Introduction

Unconventional polarization states, also known as "vector beams", are gaining increasing interest in recent years [1–9]. In contrast to conventional polarization states, such as linear, circular or elliptical polarizations, which can be uniquely described by a specific point on the surface of the Poincaré sphere [10], the vector beams, have a spatial inhomogeneous polarization state, and therefore cannot be described by a point, but rather by a number of points on the Poincaré sphere. The radial and azimuthal polarizations, for example, span the equator of the Poincaré sphere. Recently the generation of vector fields with hybrid state of polarization was demonstrated [11,12]. These spatially inhomogeneous beams, coined hybrid beams (HBs), are composed of spatially separated linear, circular and elliptical polarizations and can span complete meridians on the surface of the Poincaré sphere. The propagation of such beams in a uniaxial crystal and the generation of supercontinuum optical vortex using such beams were studied and demonstrated [13,14]. In addition, Beckley et al. [15] demonstrated the generation of full Poincaré beams that span the entire surface of the Poincaré sphere in a single beam. These beams may be important in particle orientation analysis applications, microscopy and in atomic systems where different polarizations satisfy different selection rules. In this paper, we discuss and demonstrate two methods for generating hybrid beams by means of radially polarized light and a wave plate. By changing either the orientation of the wave plate, or its phase retardation, a full coverage of the Poincaré sphere

#138361 - $15.00 USD Received 17 Nov 2010; revised 10 Dec 2010; accepted 10 Dec 2010; published 15 Dec 2010

can be achieved. Furthermore, we analyze the focal plane field and energy density distribution of these HBs when focused by a high numerical aperture (NA) lens and we discuss their possible applications.

2. Theoretical background

In the Poincaré sphere representation, the Stokes parameters s_1, s_2, s_3 are regarded as the Cartesian coordinates of a point **P** on the sphere with radius s_0 (representing constant intensity). The spherical angular coordinates of the sphere are 2χ and 2ψ so that each point on the sphere corresponds to a unique state of polarization of a plane monochromatic wave (see Fig. 1(a)) [10]. The HB, as we shall refer to in this paper, spans a closed circle on the surface of the Poincaré sphere whose center coincides with the center of the sphere. Therefore, in the context of this paper, the radial polarization can be thought of as a specific case of the HB.

Next we discuss two methods for generating HB using a radially polarized light and a wave plate. In the first method, we start with the generation of radially polarized light, which can be achieved using variety of approaches [16–21]. Specifically for our experiment we do so using either a subwavelength grating element [22] or a liquid crystal element [23]. Next, the radially polarized light is transmitted through a quarter wave plate (QWP), where its orientation (defined by its major axis) can be rotated with regard to the x axis. The QWP changes the state of polarization in such a way that its projection on the Poincaré sphere no longer spans the equator of the sphere. Instead, it spans a complete meridian crossing the two poles of the sphere. The latitude angle 2ψ of the spanned meridian is determined by the angle of the QWP, so continuously rotating the QWP by $\pi/2$ radians with regard to its starting position scans the complete surface of the Poincaré sphere. Figure 1(b) shows an example of the polarization field obtained by transmitting a radially polarized light through a QWP oriented in 45 degrees with respect to the x axis. Figure 1(c) shows the projections on the Poincaré sphere of such HBs with different orientations of the QWP. Rotating the QWP, results in rotation of the projected circle on the sphere around the axis connecting the north and the south poles of the sphere.

Similarly to the first approach, the second method is also based on transmitting a radially polarized light through a wave plate. However, the wave plate orientation is now fixed, and its phase retardation can be modulated, e.g. by using a liquid crystal cell. In this case the projection of the polarization field on the Poincaré sphere is a closed circle having the same center as the sphere, which crosses the equator at two opposite points. Changing the phase retardation of the plate, results in rotation of the projected circle on the sphere around the axis connecting the two opposite points on the equator. Therefore, changing the retardation of the plate from 0 to π radians scans the complete surface of the Poincaré sphere. Figure 1(d) shows the projections on the Poincaré sphere of such HBs with different phase retardation of the phase plate. The orientation of the rotation axis on the plane of the equator is determined by the orientation of the wave plate.

Next we cast this discussion in a mathematical form. The general Jones vector for the electric field of a radial polarization transmitted through a wave plate is given by

$$\vec{E} = T_{wp} \cdot V_r \tag{1}$$

Where, $T_{wp} = \begin{pmatrix} e^{-i\frac{\Gamma}{2}}\cos^2(\psi) + e^{i\frac{\Gamma}{2}}\sin^2(\psi) & -i\sin(\frac{\Gamma}{2})\sin(2\psi) \\ -i\sin(\frac{\Gamma}{2})\sin(2\psi) & e^{-i\frac{\Gamma}{2}}\sin^2(\psi) + e^{i\frac{\Gamma}{2}}\cos^2(\psi) \end{pmatrix}$ is the Jones matrix of a wave plate with retardation Γ oriented at an angle ψ with respect to the x axis, and

#138361 - $15.00 USD Received 17 Nov 2010; revised 10 Dec 2010; accepted 10 Dec 2010; published 15 Dec 2010

$V_r = \begin{pmatrix} \cos(\theta) \\ \sin(\theta) \end{pmatrix}$ is the Jones vector of the radially polarized light, where θ is the azimuthal angle in polar coordinate system.

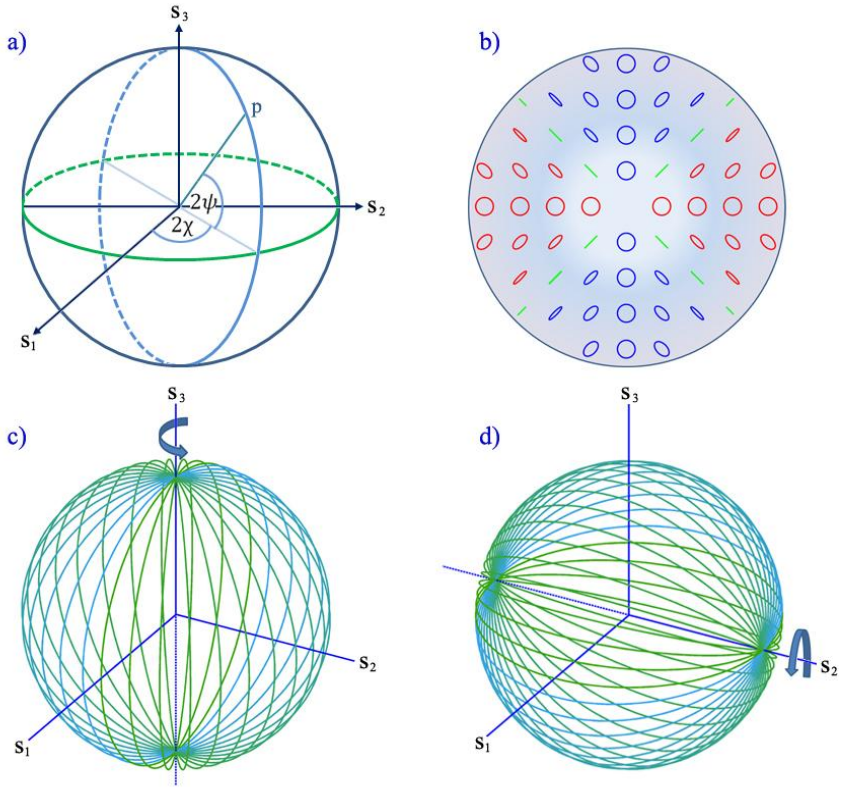

Fig. 1. (a) Standard Poincaré sphere representation of a polarization state. The radially polarized field spans the equator of the sphere (b) polarization distribution obtained by transmitting a radially polarized light through a QWP oriented at 45 degrees with respect to the x axis. Blue – right handed polarization, red– left handed polarization, green – linear polarization. (c) HBs projections on the Poincaré sphere, where each circle corresponds to a different orientation of the QWP used to generate these beams. (d) HBs projections on the Poincaré sphere, where each circle corresponds to a different phase retardation of the wave plate used to generate these beams.

Using these expressions we obtain

$$\vec{E} = \begin{pmatrix} \cos(\theta)\cos(\frac{\Gamma}{2}) - i\sin(\frac{\Gamma}{2})\cos(2\psi - \theta) \\ \sin(\theta)\cos(\frac{\Gamma}{2}) - i\sin(\frac{\Gamma}{2})\sin(2\psi - \theta) \end{pmatrix} \quad (2)$$

This is a general expression from which the Stokes parameters can be calculated. When projected on the Poincaré sphere this electric field spans a closed circle whose center coincides with the center of the sphere. For example, setting $\Gamma = \pi/2$ and $\psi = 0$ represents a case of a radially polarized beam transmitted through a QWP oriented along the x axis. The Stokes parameters in this case are $S_0 = 1, S_1 = \cos(2\theta), S_2 = 0, S_3 = \sin(2\theta)$ and its projection on the Poincaré sphere spans a closed circle in the plane defined by the S_1 and S_3 vectors.

#138361 - $15.00 USD Received 17 Nov 2010; revised 10 Dec 2010; accepted 10 Dec 2010; published 15 Dec 2010

3. Experimental results

In order to demonstrate the generation and characterization of such HBs we used the first proposed method. First we used a liquid crystal polarization converter (Arcoptix, Switzerland) to convert the linearly polarized beam emerging from a1064 nm Nd:YAG laser into a radially polarized beam. The emerging radially polarized light illuminates a rotatable QWP followed by a rotatable linear polarizer, and is then imaged onto a charge coupled device (CCD) camera. Figures 2 (a) and (b) show a schematic representation of the polarization distributions that would be obtained with the QWP oriented at 45 and 0 degrees with respect to the x axis, respectively. Figures 2 (c) and (d) show the intensity distribution of these two HBs, after being transmitted through the analyzer whose orientation is indicated by the arrows. The obtained intensity is given by multiplying the field (Eq. (2) by the Jones matrix of an analyzer, oriented at an angle φ with respect to the x axis.

$$I = \cos^2(\frac{\Gamma}{2})\cos^2(\phi-\theta)+\sin^2(\frac{\Gamma}{2})\cos^2(\phi-2\psi+\theta) \qquad (3)$$

As can be seen, the obtained intensity pattern varies from a constant intensity with zero contrast along the azimuthal direction, to a high contrast pattern along that same direction. The orientation of the bright and dark zones is determined by the angles of the QWP and the analyzer. The period of this orientation rotation is $\pi/2$.

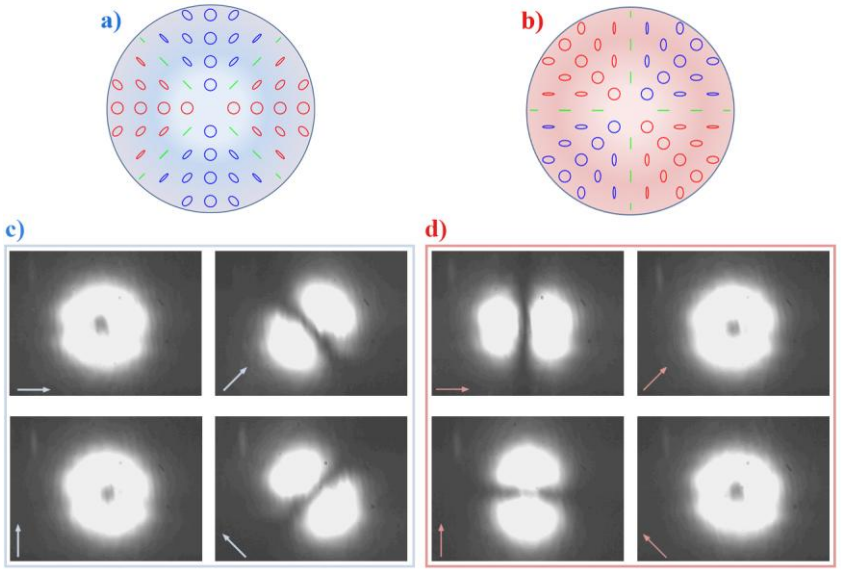

Fig. 2. (a) and (b) schematics of polarization distributions that would be obtained by a radially polarized field transmitted through a QWP oriented at 45 and 0 degrees, respectively. (c) and (d) pictures of the experimentally generated fields of (a) and (b) respectively, being transmitted through an analyzer. The arrows show the orientation of the analyzer.

4. Tight focusing numerical analysis

One aspect of the vectorial beams that was extensively studied in recent years is their field distribution near the focus of a high NA lens and focal field design by polarization distribution manipulation [24–32]. Here we use the method of Richards and Wolf [33], (originally developed for linear polarization) to study the energy density and the field distribution of the HB in a wavelength scale volume near the focus. Calculating the distribution of energy density at the focal plane for circular polarization illumination is performed by decomposing

#138361 - $15.00 USD Received 17 Nov 2010; revised 10 Dec 2010; accepted 10 Dec 2010; published 15 Dec 2010

the circular polarization into two orthogonal linear polarizations with equal amplitudes and a π/2 phase difference between them. Thus, one has to sum the focal field due to an incident x polarization together with the focal field due to an incident y polarization with a π/2 phase difference. Similarly, an elliptically polarized light can be decomposed into two orthogonal linear polarizations with different amplitudes and with the specific phase difference between them. Following a procedure similar to that of a circular polarization, the distribution of energy density in the focal plane is given by adding the contributions from the two orthogonal polarization states with the specific phase difference. Further details regarding adding the contributions of the orthogonal polarizations are given in [34]. Following that procedure, we decomposed the field of the HB at every pixel to its x and y components and obtained x and y polarized fields with spatially varying amplitudes and phases. We calculated the focal plane field components due to these two fields and then sum up the fields to obtain the total energy density distribution. As an example, Fig. 3(a) shows the energy density distribution at the focal plane of a NA = 0.94 lens illuminated with the HB shown in Fig. 2(a). The beam propagates along the z direction. By a careful choice of the NA, a rectangular flattop shape is obtained at the focus. As can be seen, all the three field components have non-negligible amplitude at the focal plane. In addition, the relative phases between these three components vary in space as a consequence of the HB illumination. Therefore, a distinctive polarization distribution is created in the focal plane, with space variant ellipticity and 3D orientation, i.e. the orientation of these polarizations ellipses is not bounded to the x-y plane, rather it can be oriented at any direction in the 3D space. The polarization ellipses at the focal plane are shown in Fig. 3(b). Figure 3(c) shows the cross section through the center of Fig. 3(b). Figures 3(d) and 3(e) show the polarization projections on the x-y and x-z planes, respectively. It can be seen that near the center of the beam, the polarization ellipses are strongly oriented along the z axis due to the strong z field component that is present around the focus.

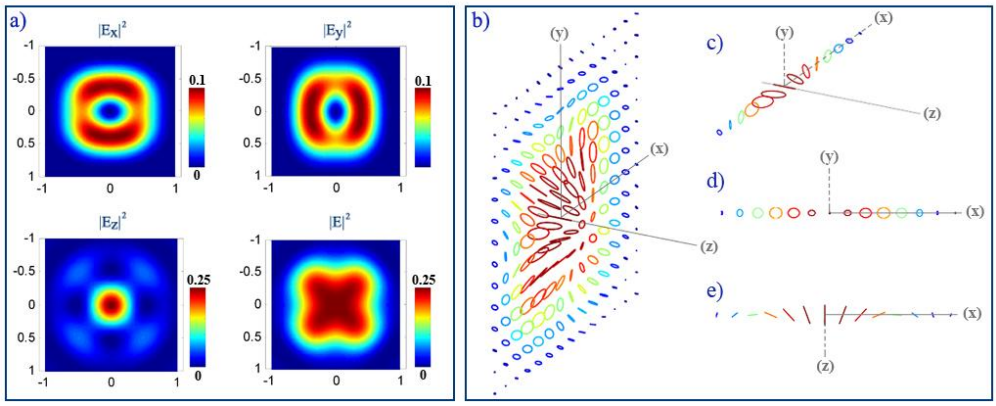

Fig. 3. (a) Energy density components and the total energy density at the focal plane of a NA = 0.94 lens illuminated by the HB of Fig. 2(a). (b) The polarization ellipses at the focal plane having a 3D orientation distribution (Media 1). The colors are related to the total energy density at the focus. (c) Cross sections through the center of (b). (d) and (e) polarization projections on the x-y and the x-z planes, respectively.

Media 1 shows the evolution of the polarization distribution and the energy density as the HB propagates through the focal plane. For visualization purposes, each frame of this media is normalized separately. It can be seen that the z polarization component increases near the focal plane and disappears when the beam is about one wavelength far from the focal plane. The depth of focus of that HB can be estimated from Fig. (4) where the energy density is plotted as a function of the x and the z coordinates.

#138361 - $15.00 USD Received 17 Nov 2010; revised 10 Dec 2010; accepted 10 Dec 2010; published 15 Dec 2010

5. Discussion

Generation of HBs, and the ability to scan the whole Poincaré sphere may find applications in microscopy and particles manipulation. For example, Ref [35]. demonstrated the mapping of the focal field components using single fluorescent molecules. The fluorescence rate of a molecule is proportional to the square of the vector multiplication of the absorption dipole moment and the illumination electric field vector. Therefore, the fluorescence pattern of differently oriented molecules reveals the various field components at the focal plane. The same experiment can be used vice versa. The a priori knowledge of the focal field components of the HBs, together with the molecules fluorescent pattern, can be used to determine the molecules orientation in the 3D space. Since the three field components of a HB at the focal plane are comparable in amplitude, significant signal can be obtained from molecules oriented along any arbitrary direction using a single shot illumination. The ability to quickly scan the Poincaré sphere can be used to find the specific polarization in which the molecular excitation is maximal and then tune the illumination light into that polarization state, to enhance the emission rate of the molecules. The same concept can be used to align molecules with dipole moment along the different field components. Another example is the interaction of the HB with chiral molecules. Such molecules absorb elliptically polarized light as a function of their chirality and orientation with respect to the orientation of the elliptically polarized light. The HBs may also find applications in atomic systems where different polarizations satisfy different selection rules. For instance, the selection rule between hyperfine states with quantum magnetic numbers M_F is $\Delta M_F = 0$ for linear polarization, $\Delta M_F = 1$ for right hand circular polarization and $\Delta M_F = -1$ for left hand polarization. By using the HBs one can excite the atomic system state population, with all the above mentioned selection rules simultaneously. This technique may be useful for spatial imaging of the atomic state of atoms [36]. In particular we believe that this approach may be plausible for cold atoms due to their distinct spatial distribution.

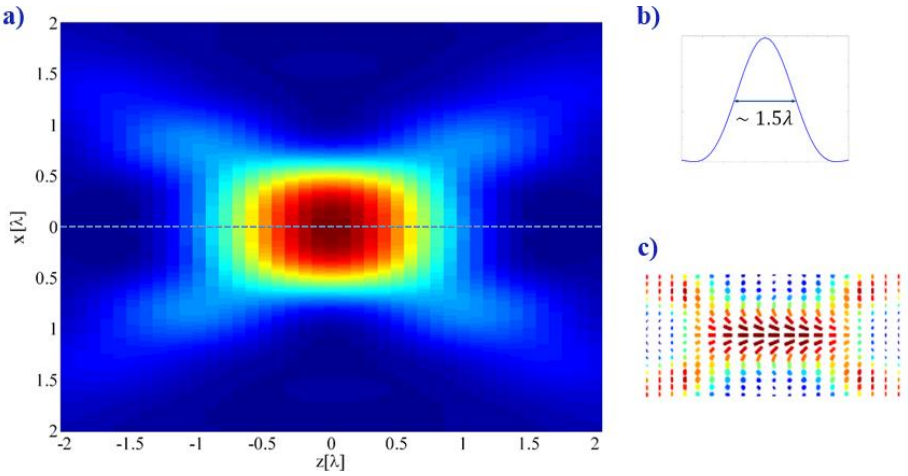

Fig. 4. (a) Calculated energy density in the x-z plane. (b) The cross section of the energy density along the dashed line in (a). (c) Consecutive polarization projections on the x-z plane demonstrating the evolution of the polarization distribution as the beam propagates through the focal plane. All calculations were performed for a NA = 0.94 lens.

6. Summary

In summary, we discussed two methods for the generation of hybrid beams, whose polarization projection spans a closed circle on the surface of the Poincaré sphere whose center coincides with the center of the sphere. The first approach is based on rotating a quarter wave plate while the second approach is based on controlling the phase retardation of a wave

#138361 - $15.00 USD Received 17 Nov 2010; revised 10 Dec 2010; accepted 10 Dec 2010; published 15 Dec 2010

plate. We demonstrated experimentally the construction of such beams and found the obtained polarization distribution in agreement with the theoretical prediction. In addition we numerically investigated the field and energy density distribution across the focal plane of a high NA lens illuminated by a hybrid beam. The results show an interesting polarization distribution with 3D orientation and space variant ellipticity. This kind of polarization distributions hold a promise in particle orientation analysis applications, microscopy and in atomic systems where different polarizations satisfy different selection rules.

Acknowledgments

G. M. Lerman gratefully acknowledges the support of the Eshkol Fellowship. L. Stern gratefully acknowledges the support of the Peter Brojde Center for Innovative Engineering and Computer Science.

#138361 - $15.00 USD Received 17 Nov 2010; revised 10 Dec 2010; accepted 10 Dec 2010; published 15 Dec 2010